

Long-term depression of climbing fiber-evoked calcium transients in Purkinje cell dendrites

John T. Weber*, Chris I. De Zeeuw*, David J. Linden†, and Christian Hansel**

*Department of Neuroscience, Erasmus MC, 3000 DR, Rotterdam, The Netherlands; and †Department of Neuroscience, The Johns Hopkins University School of Medicine, Baltimore, MD 21205

Edited by Charles F. Stevens, The Salk Institute for Biological Studies, La Jolla, CA, and approved January 14, 2003 (received for review October 22, 2002)

In recent years much has been learned about the molecular requirements for inducing long-term synaptic depression (LTD) in various brain regions. However, very little is known about the consequences of LTD induction for subsequent signaling events in postsynaptic neurons. We have addressed this issue by examining homosynaptic LTD at the cerebellar climbing fiber (CF)-Purkinje cell (PC) synapse. This synapse is built for reliable and massive excitation: Activation of a single axon produces an unusually large α -amino-3-hydroxy-5-methyl-4-isoxazole propionic acid receptor-mediated synaptic current, the depolarization of which drives a regenerative complex spike producing a large, widespread Ca^{2+} transient in PC dendrites. Here we test whether CF LTD has an impact on dendritic, complex spike-evoked Ca^{2+} signals by simultaneously performing long-term recordings of complex spikes and microfluorimetric Ca^{2+} measurements in PC dendrites in rat cerebellar slices. Our data show that LTD of the CF excitatory postsynaptic current produces a reduction in both slow components of the complex spike waveform and complex spike-evoked dendritic Ca^{2+} transients. This LTD of dendritic Ca^{2+} signals may provide a neuroprotective mechanism and/or constitute "heterosynaptic metaplasticity" by reducing the probability for subsequent induction of those forms of use-dependent plasticity, which require CF-evoked Ca^{2+} signals such as parallel fiber-PC LTD and interneuron-PC LTP.

In the adult mammalian brain, Purkinje cells (PCs) receive two types of excitatory synaptic input: (i) from numerous parallel fibers (PFs), which are the axons of granule cells, and (ii) from a single climbing fiber (CF), which originates from the inferior olive. The PFs primarily form synaptic contacts at the distal compartments of the PC dendrite as well as at spiny branchlets of more proximal compartments, whereas the CF predominately contacts the proximal compartment at the primary dendrite via spines found in this region at low density (1–3). The CF input is extremely powerful, consisting of $\approx 1,400$ release sites (4) that are characterized by a high release probability (5, 6). Accordingly, CF activation produces a strong postsynaptic depolarization that is mediated by α -amino-3-hydroxy-5-methyl-4-isoxazole propionic acid (AMPA) receptors and evokes an all-or-none spike with multiple peaks. These "complex spikes" are accompanied by a large Ca^{2+} transient covering broad regions of the PC dendritic tree (7–10). Complex spikes, as recorded at the soma, are characterized by an initial, fast spike component followed by a series of smaller spikelets riding on top of a plateau. It has been suggested that the fast component is a somatically generated Na^+ spike, whereas the following slower components are produced mainly by dendritic Ca^{2+} conductances (11, 12). More recently it has been shown that isolated PC somata can fire repetitive spike patterns on their own that are mediated by a "resurgent" Na^+ current (13). Thus, it is likely that both Ca^{2+} and Na^+ currents contribute to the slow-complex spike components (see ref. 14 for review).

In Marr-Albus-Ito models of cerebellar function (15–17), long-term depression (LTD) at the PF-PC synapses provides a cellular substrate of some forms of cerebellar motor learning. PF LTD can be induced by simultaneous PF and CF activation at low frequencies (18). In these models, the CF is considered invariant and provides a "teacher signal" that is activated when a need for

adaptive learning emerges. At the cellular level, the contribution of CF activity to PF-LTD induction consists of the dendritic Ca^{2+} transient (9), which leads to supralinear Ca^{2+} signals when the CF and PF are simultaneously activated (19). Furthermore, it has been suggested that corticotropin-releasing factor, released from CF terminals, might play a permissive role in PF-LTD induction (20). At the PF input, both metabotropic glutamate receptor 1 and AMPA receptors must be activated. Downstream of these initial signals, there is a requirement for the activation of protein kinase C (PKC) (21–23), ultimately resulting in the internalization of AMPA receptors (refs. 24 and 25; see ref. 26 for review).

Recently we demonstrated that LTD could also be obtained at the CF-PC synapse after a 30-s, 5-Hz CF tetanization (ref. 27; see also ref. 28). CF LTD was characterized by a reduction in the amplitude of excitatory postsynaptic currents (EPSCs) recorded in voltage-clamp mode. Similar to PF LTD, it depended on a rise in Ca^{2+} levels, the activation of metabotropic glutamate receptor 1, and the activation of PKC. It seems to be expressed postsynaptically, because it is not associated with an alteration in the synaptic glutamate transient (29). Moreover, it was shown that application of the same stimulus protocol resulted in a selective reduction of slow-complex spike components when recordings were conducted in current-clamp mode. Although the initial Na^+ spike was unaffected, there was a reduction in the amplitude of slow spikelets; this effect was observed most reliably in the case of the first slow-spike component (27).

What impact can the observed reduction of $\approx 20\%$ in the EPSC amplitude and a similar modest reduction in a slow spikelet have at a type of synapse that seems to operate with an unusually high safety factor? We hypothesize that despite the large suprathreshold nature of the complex spike, CF LTD results in a persistent reduction of CF-evoked dendritic Ca^{2+} transients and have tested this hypothesis by performing simultaneous whole-cell patch-clamp recording and microfluorimetric Ca^{2+} imaging while inducing and monitoring LTD at the CF-PC synapse.

Materials and Methods

Slice Preparation and Electrophysiology. Sagittal slices of the cerebellar vermis (200 μm thick) were prepared from postnatal-day 18–28 Sprague–Dawley rats by using a Vibratome and standard artificial cerebrospinal fluid containing 124 mM NaCl, 5 mM KCl, 1.25 mM Na_2HPO_4 , 2 mM MgSO_4 , 2 mM CaCl_2 , 26 mM NaHCO_3 , and 10 mM D-glucose bubbled with 95% O_2 /5% CO_2 . After a recovery period of at least 1 h, the slices were placed in a submerged chamber that was perfused at a flow rate of 3 ml/min with room-temperature artificial cerebrospinal fluid supplemented with 20 μM bicuculline methiodide to block γ -aminobutyric acid type A receptors. Recording was performed by using the visualized whole-cell patch-clamp technique with a Zeiss Axioskop FS and either an

This paper was submitted directly (Track II) to the PNAS office.

Abbreviations: PC, Purkinje cell; PF, parallel fiber; CF, climbing fiber; AMPA, α -amino-3-hydroxy-5-methyl-4-isoxazole propionic acid; LTD, long-term depression; EPSC, excitatory postsynaptic current; BAPTA, 1,2-bis(2-aminophenoxy)ethane- N,N,N',N' -tetraacetic acid; NBQX, 1,2,3,4-tetrahydro-6-nitro-2,3-dioxo-benzo-[f]quinoxaline-7-sulfonamide.

*To whom correspondence should be addressed. E-mail: c.hansel@erasmusmc.nl.

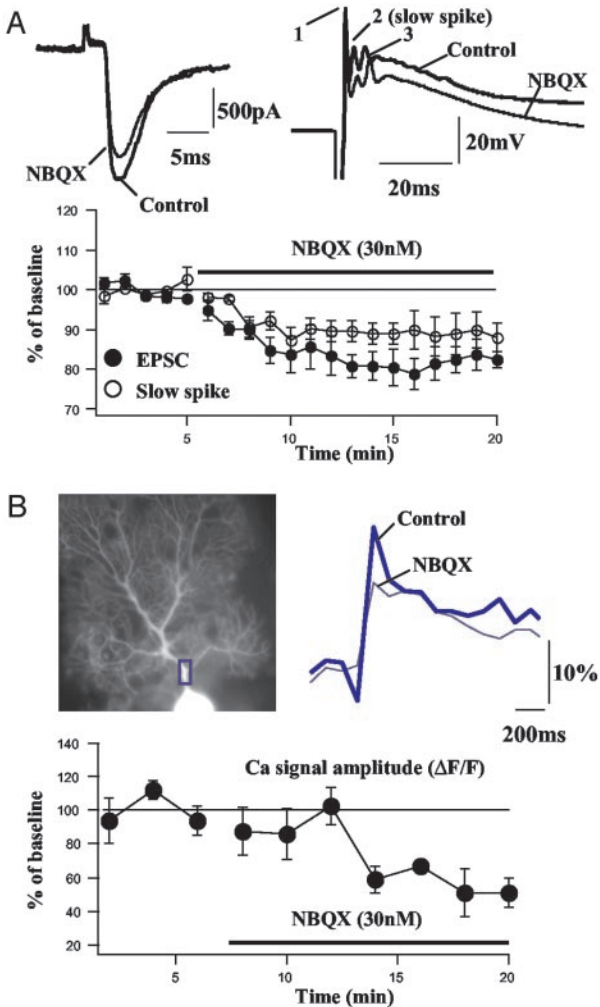


Fig. 1. Complex spike modification is produced by a dose of the AMPA receptor antagonist NBQX designed to mimic CF LTD. (A *Upper Left*) Representative CF EPSC elicited by a single test pulse under control conditions and in the presence of 30 nM NBQX. Tracings are representative of five cells. (A *Upper Right*) Representative complex spike elicited by a single test pulse under control conditions and in the presence of 30 nM NBQX. For simplicity, the second spike is termed “slow spike.” Tracings are representative of five cells. (A *Lower*) Averaged EPSC ($n = 5$) and slow-spiking amplitude changes ($n = 5$). (B *Upper*) Representative image and Ca^{2+} transients in the presence of NBQX. (B *Lower*) Averaged changes in the Ca^{2+} signal amplitude ($n = 3$).

Axoclamp 2A amplifier (Axon Instruments, Foster City, CA) or an EPC-8 amplifier (HEKA Electronics, Lambrecht/Pfalz, Germany). For the majority of experiments, the recording electrodes (resistance 2.5–4 M Ω) were filled with a solution containing 9 mM KCl, 10 mM KOH, 120 mM K gluconate, 3.48 mM MgCl₂, 10 mM Hepes, 4 mM NaCl, 4 mM Na₂ATP, 0.4 mM Na₃GTP, and 17.5 mM sucrose (pH 7.25). For the EPSC recordings shown in Fig. 2, the electrodes were filled with a Cs-based solution containing 128 mM CsOH, 111 mM gluconic acid, 4 mM NaOH, 10 mM CsCl, 2 mM MgCl₂, 10 mM Hepes, 4 mM Na₂ATP, 0.4 mM Na₃GTP, and 30 mM sucrose (pH 7.25). In some experiments, Oregon green BAPTA-2 (200 μ M) was added to the internal saline. All drugs were purchased from Sigma except for Oregon green BAPTA-2 (Molecular Probes). When the Axoclamp 2A amplifier was used, currents were filtered at 2 kHz, digitized at 20 kHz, and acquired by using AXODATA software. When the EPC-8 was used, currents were filtered at 3 kHz, digitized at 3.8 kHz, and acquired by using PULSE software. During voltage-clamp recordings, holding poten-

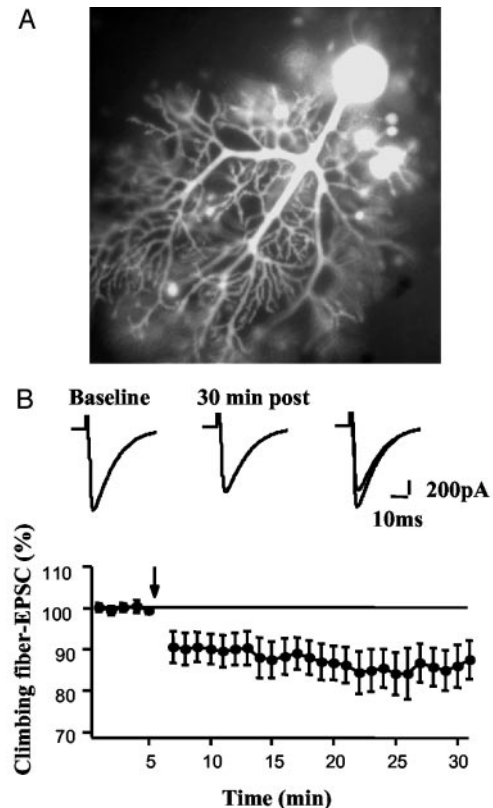


Fig. 2. LTD of CF EPSCs in the presence of Oregon green BAPTA-2. (A) Representative image of a PC filled with 200 μ M Oregon green BAPTA-2. (B *Upper*) CF EPSCs during baseline and 30 min after tetanization (5 Hz \times 30 s). (B *Lower*) Summary of CF EPSC amplitudes in five cells tetanized in the presence of the dye. The tetanus onset is indicated by the downward arrow.

tials were chosen in the range of -40 to -10 mV to inactivate voltage-gated Na⁺ and Ca²⁺ channels (for more details see ref. 27). During current-clamp recordings, small negative currents were passed to move the PC in the range of -75 to -65 mV to prevent spontaneous spike activity. For extracellular stimulation, standard patch pipettes were used that were filled with external saline. CFs were stimulated in the granule cell layer. Test responses were evoked at a frequency of 0.05 Hz by using ≈ 3 - μ A pulses that were applied for 500 μ s. Our major goal for the long-term recordings was to monitor possible changes in dendritic Ca²⁺ signals in correlation to changes in the complex spikes. We therefore also accepted cells that were recorded for shorter time periods than the ≥ 25 -min display chosen for the time graphs in Figs. 3–5. Only cells that were innervated by a single CF input, as indicated by a single step in the CF input-output relation, were used. To monitor complex spike waveform modifications, the amplitudes of spike components were measured as the peak amplitudes relative to a proceeding trough or the prestimulus membrane potential, chosen for each cell to maximize stability during the baseline period. Cells were excluded from the study if the input resistance varied by $>15\%$ over the course of the experiment. If not indicated otherwise, the group data are reported as mean \pm SEM in the text and represent averages over a 3-min period around the time point shown.

Calcium Imaging. After achieving the whole-cell configuration, the neurons were loaded with the Ca²⁺ indicator Oregon green BAPTA-2 (200 μ M) by diffusion from the patch pipette. The experiments were initiated after the PC dendrite was loaded adequately with the dye and the fluorescence at the regions of measurement reached a steady-state level, which typically required

CONTROL GROUP

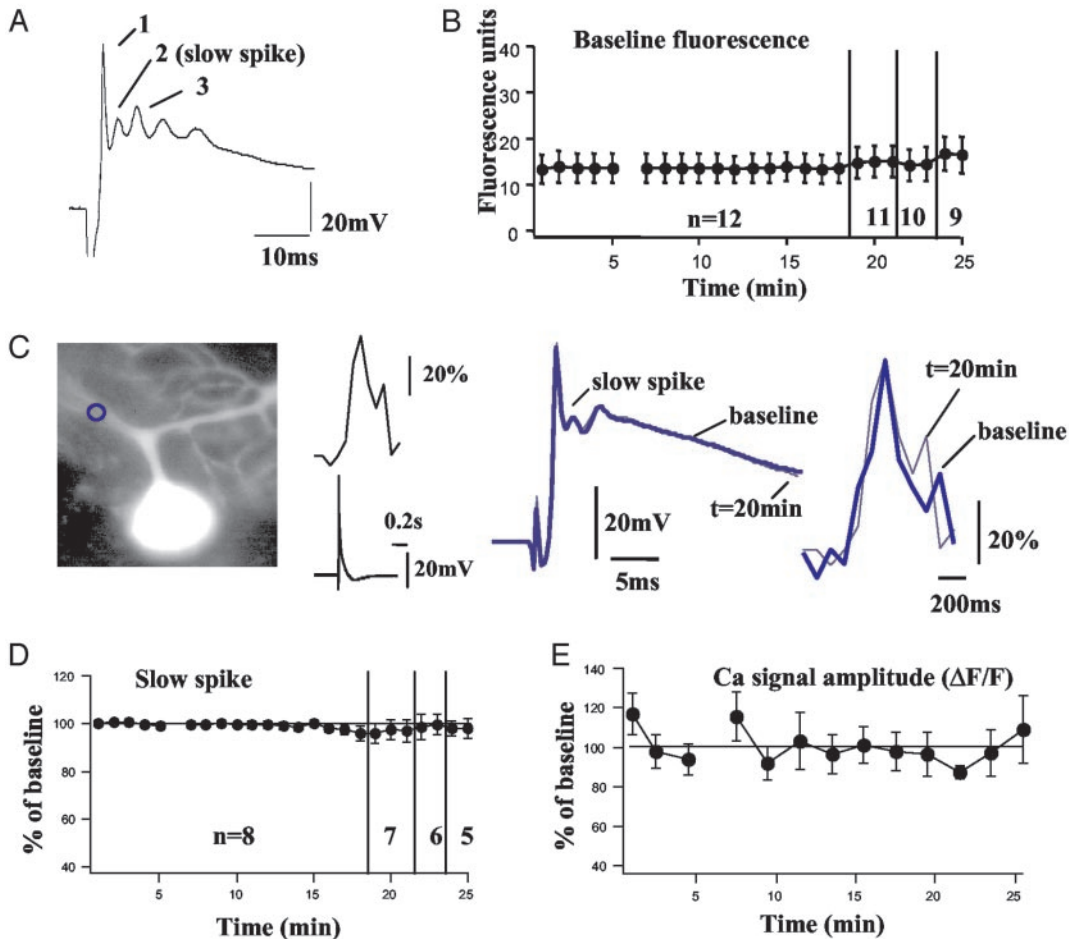


Fig. 3. Long-term recordings of complex spikes and Ca^{2+} transients under control conditions. (A) Nomenclature of complex spike components. (B) Baseline fluorescence of Oregon green BAPTA-2 measured in 12 cells (including the eight control cells). (C) Image, complex spike, and Ca^{2+} signal in a representative control cell. The thick tracings indicate complex spike and associated Ca^{2+} signal during the baseline. The thin tracings are at $t = 20$ min. Ca^{2+} signals are expressed as percentage of $\Delta F/F$ and were measured in the region of interest indicated in blue (Left). (D) Average amplitude of the slow spike in eight control cells. Data points represent the average of three successive responses. (E) Average peak amplitude of Ca^{2+} signals measured in proximal dendritic regions of the eight control cells represented in D. With the exception of the first image (uneven number of images), the data points represent the average of two successive images.

~30 min. Fluorescence was excited with a 100-W HBO lamp, the light of which was passed onto the preparation through a DX-1000 optical switch (Solemere Technology, Salt Lake City), an excitation filter (maximal transmission at 485 nm), and a $\times 40$ Achromplan objective (Zeiss). Changes in the fluorescence of Oregon green BAPTA-2 were measured after the light passed through an emission filter (maximal transmission at 530 nm) by using a cooled charge-coupled device camera (Pentamax or Quantix, both from Roper Scientific, Trenton, NJ). During the test periods, an image sequence was taken once per minute (with every third CF stimulation). Each sequence was composed of a series of 20 frames (individual exposure time was 50 ms) with an acquisition frequency in the range of 10–15 Hz (depending on the size of the selected pixel array). For data acquisition and analysis we used IPLAB software (Scanalytics, Billerica, MA). Fluorescence changes were normalized to resting levels and expressed as the ratio $\Delta F/F(t) = [F(t) - F]/F$, where $F(t)$ is the fluorescence value at time t , and F is the averaged fluorescence obtained during the baseline period preceding the stimulus application (four frames). Background fluorescence was subtracted before all quantifications. These background values were obtained from a cell-free region located close to the dye-loaded cell. The Ca^{2+} signal amplitudes were obtained by measuring the time-locked peak fluorescence value (one frame)

after stimulation. To obtain a quantification of Ca^{2+} signal amplitudes based on more than just one data point per Ca^{2+} transient, we additionally determined the average from three subsequent frames starting with the peak. In the figures, typical cell data (spikes and fluorescence signals) are averaged from 2–10 individual traces.

Results

An initial set of experiments was conducted to determine whether the complex spike modification observed after CF tetanization results from the LTD of CF EPSCs or, alternatively, whether a direct modification of voltage-dependent conductances underlying the complex spike is involved. To do so, we attempted to mimic CF LTD by reducing the EPSC amplitude with the competitive AMPA receptor antagonist 1,2,3,4-tetrahydro-6-nitro-2,3-dioxo-benzo-[f]quinoxaline-7-sulfonamide (NBQX). After stable recordings of CF EPSCs for a baseline period of ≥ 5 min, 30 nM NBQX was applied in the bath. Application of 30 nM NBQX caused a reduction of CF EPSCs (Fig. 1A) that was similar in amplitude ($82.0 \pm 3.6\%$ of baseline, measured for 5 min after NBQX was completely infused in the bath; $n = 5$) to that caused by CF tetanization (27). In separate PC recordings in current-clamp mode, application of 30 nM NBQX caused a modification of complex spikes that closely resembled that observed after CF

TETANUS GROUP

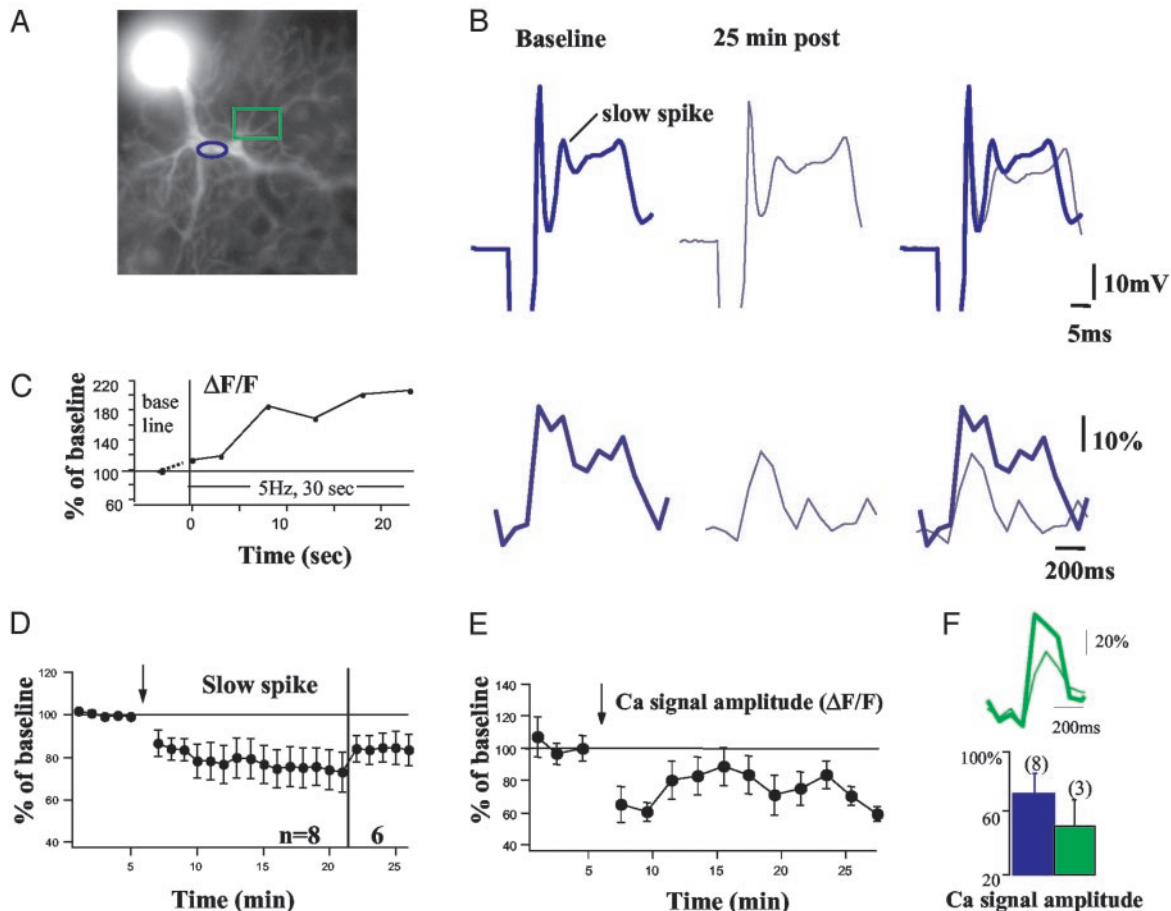


Fig. 4. Long-term recordings of complex spikes and Ca^{2+} transients in tetanized cells. (A) Representative image from a tetanized cell. (B) Representative complex spikes from the same cell with corresponding Ca^{2+} signals (blue circle) shown below (expressed as percentage of $\Delta F/F$). (C) Ca^{2+} accumulation measured in a different cell during the 30-s tetanus period. The data are shown as percentage of change relative to the averaged test $\Delta F/F$ values obtained during the baseline. (D) Average amplitude of the second spike component (slow spike) in eight tetanized cells. (E) Average peak amplitude of Ca^{2+} signals measured in proximal dendritic regions of the eight tetanized cells represented in D. (F Upper) Representative Ca^{2+} signals from spiny branchlets (green box). (F Lower) Comparison of the reduction of Ca^{2+} signal amplitudes at regions of the primary dendrite (blue, $n = 8$) and spiny branchlets (green, $n = 3$) at $t = 20$ min. All conventions are as described for Fig. 3.

tetanization (27). The amplitude of the second spike component, in this study referred to as the “slow spike,” was reduced to $89.1 \pm 5.2\%$ of baseline (measured for 5 min after complete NBQX bath infusion; $n = 5$). In three additional cells, $200 \mu\text{M}$ Oregon green BAPTA-2 was added to the internal saline, and the effect of NBQX on the amplitude of CF-evoked Ca^{2+} transients in PC dendrites was determined. The Ca^{2+} -signal amplitude was reduced to $55.2 \pm 9.5\%$ of baseline (measured for 5 min after complete NBQX bath infusion; $n = 3$; Fig. 1B). In these three cells, the slow-spike amplitude was reduced to $89.5 \pm 6.1\%$ of baseline. Activation of AMPA receptors located in spines leads to a depolarization that activates voltage-gated Ca^{2+} channels. The Ca^{2+} transient spreads through the adjoining dendritic shafts and through the extent of the PC dendritic tree (7–10). We therefore suggest that CF LTD reduces the AMPA receptor-mediated depolarization, thereby reducing voltage-dependent Ca^{2+} conductances, resulting in the observed modification of the complex spike and its associated Ca^{2+} transient.

To monitor possible changes in Ca^{2+} transients associated with CF LTD, we performed simultaneous long-term measurements of Ca^{2+} signals and complex spikes. Because Ca^{2+} indicator dyes act as Ca^{2+} buffers and thus could inhibit the Ca^{2+} -dependent CF-

LTD induction, it was necessary to first establish CF LTD in the presence of Oregon green BAPTA-2 at the concentration used later for the imaging experiments. To this end, we recorded CF EPSCs by using a Cs-based internal saline (see ref. 27) supplemented with $200 \mu\text{M}$ Oregon green BAPTA-2. After CF EPSCs (holding potential, -20 mV) remained stable for a baseline period of ≥ 5 min in PCs, the CF input was tetanized for 30 s at 5 Hz. This CF tetanization resulted in an LTD of CF EPSCs ($85.4 \pm 4.8\%$ of baseline at $t = 20$ –25 min; $n = 5$; Fig. 2). Thus, the initial experiments describing LTD of CF EPSCs ($\approx 80\%$ of baseline; see ref. 27) could be repeated in the presence of $200 \mu\text{M}$ Oregon green BAPTA-2. In contrast to these experiments, the current-clamp recordings described in the following were conducted by using a K-based saline, because we wanted to measure complex spikes under more physiological conditions. It is unlikely that the dye blocks CF LTD when this K-based saline is used, because CF LTD can also be obtained when this saline is supplemented with $200 \mu\text{M}$ BAPTA (M. Schmolesky and C.H., unpublished observation).

To investigate the stability of CF-evoked Ca^{2+} transients we simultaneously measured complex spikes and Ca^{2+} signals in regions of interest located in the proximal dendrites of PCs. In the presence of Oregon green BAPTA-2, the typical complex spike

CHELERYTHRINE GROUP

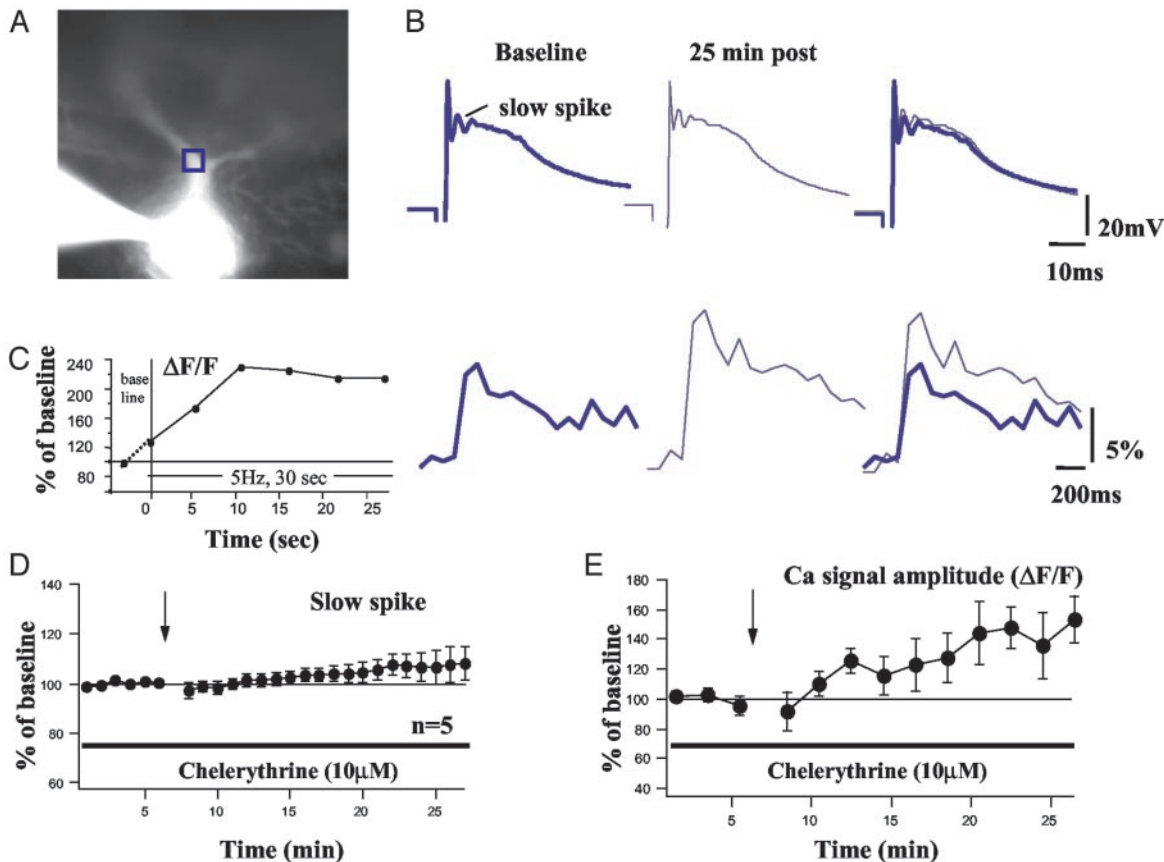


Fig. 5. Complex spikes and Ca^{2+} transients in the presence of the PKC inhibitor chelerythrine ($10 \mu\text{M}$). (A) Representative image from a cell tetanized in the presence of chelerythrine. (B) Representative complex spikes from the same cell with corresponding Ca^{2+} signals shown below (expressed as percentage of $\Delta F/F$). (C) Ca^{2+} accumulation measured in a different cell during the tetanus period. (D) Average amplitude of the slow spike in five tetanized cells in the presence of $10 \mu\text{M}$ chelerythrine. (E) Average peak amplitude of Ca^{2+} signals measured in proximal dendritic regions of the five tetanized cells represented in D. Data points are averages of two successive images. All conventions are as described for Fig. 3.

waveform could still be observed. Test pulses delivered in current-clamp mode produced multicomponent complex spikes that consisted of an initial rapid spike followed by a varying number of spikelets (1–4; Fig. 3A). To avoid artifacts in Ca^{2+} amplitude calculations based on drifts in the baseline fluorescence, this parameter was monitored constantly in regions of interest and was stable over the course of the experiments (Fig. 3B). CF stimulation reliably produced complex spike-associated Ca^{2+} transients in PC dendrites (Fig. 3C). In control cells ($n = 8$), the slow spike (Fig. 3D) was essentially unaltered when measured for 25 min ($97.2 \pm 2.3\%$ at $t = 17$ min; $n = 8$). The peak amplitude of dendritic Ca^{2+} signals (Fig. 3E) was also stable over the length of the recording period. This observation was made whether the determination of peak values was based on either one ($97.5 \pm 11.5\%$ at $t = 17$ min, $n = 8$) or three frames ($104.0 \pm 21.1\%$ at $t = 17$ min).

In cells that underwent CF tetanization, there was a reduction in both the slow-spike and the peak amplitude of dendritic Ca^{2+} signals (Figs. 4A and B). Measurement of Ca^{2+} signals during the 30-s tetanization period revealed a slow rise in Ca^{2+} in the PC dendrite that reached a plateau by the end of the tetanus period (Fig. 4C). Overall, the slow-spike component was reduced to $74.1 \pm 9.3\%$ at $t = 20$ min in tetanized cells (Fig. 4D, $n = 8$), whereas dendritic Ca^{2+} transients were reduced to $72.7 \pm 13.3\%$ at $t = 20$ min in the same cells (Fig. 4E; 3 frames, $62.6 \pm 17.5\%$). In three of the eight cells, it was possible to measure Ca^{2+} transients additionally in regions of interest at spiny dendritic branches (Fig. 4A and

F). These Ca^{2+} signals were reduced to $51.6 \pm 17.1\%$ at $t = 20$ min ($n = 3$).

In addition to a postsynaptic rise in Ca^{2+} , it has also been shown that LTD of CF EPSCs depends on the activation of PKC (27). To investigate whether the LTD of the slow-spike components and Ca^{2+} signals similarly depended on PKC activation, we conducted long-term recordings in the presence of bath-applied chelerythrine ($10 \mu\text{M}$), a potent and specific membrane-permeant inhibitor of the catalytic site of PKC. Chelerythrine was present in the bath throughout the course of the experiments. Simultaneous measurement of both complex spikes and Ca^{2+} transients in the presence of $10 \mu\text{M}$ chelerythrine did not reveal a reduction of the slow spike or the amplitude of Ca^{2+} signals after CF tetanization (Fig. 5A and B). Measurement of Ca^{2+} signals during the tetanus period in the presence of chelerythrine showed a build-up of Ca^{2+} levels (Fig. 5C) similar to that seen in the tetanized group (Fig. 4C). In addition to a blockade of CF LTD by PKC inhibition, we also observed a small increase in the slow-spike component over time (Fig. 5D; $104.6 \pm 4.0\%$ at $t = 20$ min; $n = 5$). There was an even more profound increase in Ca^{2+} signal amplitudes in the presence of chelerythrine in the same set of cells, being $138.3 \pm 19.5\%$ of baseline at $t = 20$ min (Fig. 5E; three frames, $157.6 \pm 26.3\%$). Chelerythrine alone had no marked effect on Ca^{2+} signal amplitudes ($110.7 \pm 15.0\%$ at $t = 15$ min; $n = 3$; data not shown). Tetanizing the cells in the absence or presence of chelerythrine did not result in differences in the spiking characteristics observed

during the tetanization period. The number of complex spikes evoked by 150 CF stimuli was 116 ± 19 ($n = 5$) in the presence of chelerythrine and 130 ± 10 (mean \pm SEM; $n = 8$) in its absence (as compared with 118 ± 10 ; $n = 13$; reported in ref. 27). These data show that both the reduction in the slow spikes and the attenuation of the Ca^{2+} transients depend on PKC activation. The increase in the slow-spike component and in the Ca^{2+} transients in the presence of chelerythrine is similar to observations, in which a small potentiation of the PF EPSC was observed after a blockade of PF-LTD induction by some PKC inhibitors (22). It is possible that PKC activation is not only required for the induction of both PF and CF LTD but also causes the suppression of a postsynaptic potentiating mechanism. Interestingly, in chelerythrine, the Ca^{2+} signals were potentiated more strongly than the slow spikes or the CF EPSCs (27). This might result from the fact that the dendritic Ca^{2+} transients are downstream of a local amplification process provided by voltage-dependent Ca^{2+} conductances. Thus, the amplitude of the Ca^{2+} transients might be affected to a larger degree than events upstream of this amplification process (EPSCs) or the somatically recorded complex spikes.

Discussion

Taken together, these experiments argue that LTD of the CF EPSC, a process that is PKC-dependent (27) and postsynaptically expressed (29), results in LTD of both the slow spike and the CF-evoked dendritic Ca^{2+} transient. The LTD of the slow spike and dendritic Ca^{2+} transients are likely to be a simple consequence of the reduction in CF-EPSC amplitude because (i) application of a submaximal dose of an AMPA-receptor antagonist to mimic LTD of EPSCs produced LTD of the slow spike as well as the associated Ca^{2+} transient and (ii) LTD of all three measures was blocked by a PKC inhibitor. Here we demonstrate that LTP or LTD can result in a long-term change in dendritic Ca^{2+} signaling.

Our initial observation of CF LTD (27) came as a surprise. For several reasons, synaptic transmission at CF-PC synapses was considered invariant. (i) The CF conveys information related to the unconditioned stimulus in cerebellar reflex conditioning pathways, and thus the need for plasticity at the CF input is less apparent than at PF synapses (28). (ii) The release probability at CF terminals is very high (5, 6). (iii) CF activity evokes an all-or-none response in PCs (30). Thus, it seems that CF transmission has a very high safety factor, and an $\approx 20\%$ reduction in EPSC amplitude might be expected to have no functional consequence. However, here we show that one consequence of CF LTD is a long-term alteration in dendritic Ca^{2+} transients accompanying the modification of the complex spike waveform.

A few previous studies in neurons have monitored long-term Ca^{2+} changes during certain physiological (31, 32) and pathological

conditions (33). For example, forms of LTD of γ -aminobutyric acid-mediated Ca^{2+} transients (31) and of Ca^{2+} transients evoked by excitatory activity (32) have been reported in response to the application of neuropeptide Y. For these changes in Ca^{2+} signaling, Van den Pol *et al.* (32) have introduced the term "LTD_{Ca}." Our study adds to these reports by showing that use-dependent synaptic plasticity can also result in LTD of dendritic Ca^{2+} transients.

In cerebellar PCs, LTD of dendritic CF-evoked Ca^{2+} transients might have important functional implications. In the short term, the CF-evoked Ca^{2+} transient activates Ca^{2+} -sensitive K⁺ channels, giving rise to a brief pause in ongoing PC simple spiking, which has been suggested to be important in motor control. In the long term, LTD of CF-evoked Ca^{2+} transients might be important, because these are trigger signals for synaptic gain changes at different types of synaptic inputs to PCs. For example, the CF-evoked dendritic Ca^{2+} transient is a necessary factor for the induction of LTD at PF synapses (9). We could demonstrate a long-term reduction in the amplitude of the Ca^{2+} transient not only in the primary dendrite, the contact site of CF synapses, but also in three cells directly at spiny branchlets, which are typically contacted by PFs. Given the suggestion that PF LTD underlies certain forms of motor learning (15–17, 23), CF LTD may ultimately have an effect at the behavioral level. CF-evoked Ca^{2+} signals are not only required for PF-LTD induction but also for the induction of LTP of interneuron-PC synapses (34), and thus CF LTD could alter the induction probability of this phenomenon as well. It will be useful to address these questions experimentally by comparing the CF-evoked pause, PF LTD, or interneuron-PC LTP after CF LTD induction.

Another possibility is that a reduction in CF-evoked Ca^{2+} signaling in the PC may provide a neuroprotective mechanism. This has been suggested for PF LTD (35, 36). This hypothesis is even more attractive at the CF input because it has been shown that prolonged periods of CF firing at elevated frequencies can lead to PC death (37) despite the high Ca^{2+} -buffering capacity of these cells (38). A long-term reduction in Ca^{2+} signals thus may provide a mechanism by which PCs adapt to handle a potentially high Ca^{2+} load.

We thank M. Schmolesky for critically reading the manuscript. This work was supported by The Netherlands Organization for Scientific Research, Medical and Health Research (to J.T.W. and C.I.D.Z.), a European Economic Community grant (to C.I.D.Z.), U.S. Public Health Service Grants MH51106 and MH01590 and the Develbiss Fund (to D.J.L.), The Netherlands Organization for Scientific Research, Earth and Life Sciences Grants 810-37-003 and 812-07-006 (to C.H.), and the Royal Dutch Academy of Sciences (to C.H.).

1. Ichikawa, R., Miyazaki, T., Kano, M., Hashikawa, T., Tatsumi, H., Sakimura, K., Mishina, M., Inoue, Y. & Watanabe, M. (2002) *J. Neurosci.* **22**, 8487–8503.
2. Morando, L., Cesa, R., Rasetti, R., Harvey, R. & Strata, P. (2001) *Proc. Natl. Acad. Sci. USA* **98**, 9954–9959.
3. Rossi, F., van der Want, J. J. L., Wiklund, L. & Strata, P. (1991) *J. Comp. Neurol.* **308**, 536–554.
4. Strata, P. & Rossi, F. (1998) *Trends Neurosci.* **21**, 407–413.
5. Dittman, J. S. & Regehr, W. G. (1998) *J. Neurosci.* **18**, 6147–6162.
6. Silver, R. A., Momiyama, A. & Cull-Candy, S. G. (1998) *J. Physiol. (London)* **510**, 881–902.
7. Ross, W. N. & Werman, R. (1987) *J. Physiol. (London)* **389**, 319–336.
8. Knöpfel, T., Vrana, I., Staub, C. & Gähwiler, B. H. (1991) *Eur. J. Neurosci.* **3**, 343–348.
9. Konnerth, A., Dreessen, J. & Augustine, G. J. (1992) *Proc. Natl. Acad. Sci. USA* **89**, 7051–7055.
10. Miyakawa, H., Lev-Ram, V., Lasser-Ross, N. & Ross, W. N. (1992) *J. Neurophysiol.* **68**, 1178–1189.
11. Llinás, R. & Sugimori, M. (1980) *J. Physiol. (London)* **305**, 171–195.
12. Llinás, R. & Sugimori, M. (1980) *J. Physiol. (London)* **305**, 197–213.
13. Raman, I. M. & Bean, B. P. (1997) *J. Neurosci.* **17**, 4517–4526.
14. Schmolesky, M. T., Weber, J. T., De Zeeuw, C. I. & Hansel, C. (2002) *Ann. N.Y. Acad. Sci.* **978**, 359–390.
15. Marr, D. (1969) *J. Physiol. (London)* **202**, 437–470.
16. Albus, J. S. (1971) *Math. Biosci.* **10**, 25–61.
17. Ito, M. (1984) *The Cerebellum and Neural Control* (Raven, New York).
18. Ito, M., Sakurai, M. & Tongroach, P. (1982) *J. Physiol. (London)* **324**, 113–134.
19. Wang, S.-H., Denk, W. & Häusser, M. (2000) *Nat. Neurosci.* **3**, 1266–1273.
20. Miyata, M., Okada, D., Hashimoto, K., Kano, M. & Ito, M. (1999) *Neuron* **22**, 763–775.
21. Crépel, F. & Krupa, M. (1988) *Brain Res.* **458**, 397–401.
22. Linden, D. J. & Connor, J. A. (1991) *Science* **254**, 1656–1659.
23. De Zeeuw, C. I., Hansel, C., Bian, F., Koekkoek, S. K. E., van Alphen, A. M., Linden, D. J. & Oberdick, J. (1998) *Neuron* **20**, 495–508.
24. Wang, Y. T. & Linden, D. J. (2000) *Neuron* **25**, 635–647.
25. Xia, J., Chung, H. J., Wihler, C., Huganir, R. L. & Linden, D. J. (2000) *Neuron* **28**, 499–510.
26. Bear, M. F. & Linden, D. J. (2001) In *Synapses*, eds. Cowan, W. M., Südhof, T. C. & Stevens, C. F. (Johns Hopkins Univ. Press, Baltimore), pp. 455–517.
27. Hansel, C. & Linden, D. J. (2000) *Neuron* **26**, 473–482.
28. Hansel, C., Linden, D. J. & D'Angelo, E. (2001) *Nat. Neurosci.* **4**, 467–475.
29. Shen, Y., Hansel, C. & Linden, D. J. (2002) *Nat. Neurosci.* **5**, 725–726.
30. Eccles, J. C., Llinás, R., Sasaki, K. & Voorhoeve, P. E. (1966) *J. Physiol. (London)* **182**, 297–315.
31. Obriant, K. & van den Pol, A. N. (1996) *J. Neurosci.* **16**, 3521–3533.
32. Van den Pol, A. N., Obriant, K., Chen, G. & Belousov, A. B. (1996) *J. Neurosci.* **16**, 5883–5895.
33. Weber, J. T., Rzgialinski, B. A., Willoughby, K. A., Moore, S. F. & Ellis, E. F. (1999) *Cell Calcium* **26**, 289–299.
34. Kano, M., Rexhausen, U., Dreessen, J. & Konnerth, A. (1992) *Nature* **356**, 601–604.
35. De Schutter, E. (1995) *Trends Neurosci.* **18**, 291–295.
36. Llinás, R., Lang, E. J. & Welsh, J. P. (1997) *Learn. Mem.* **3**, 445–455.
37. O'Hearn, E. & Molliver, M. E. (1997) *J. Neurosci.* **17**, 8828–8841.
38. Fierro, L. & Llano, I. (1996) *J. Physiol. (London)* **496**, 617–625.